

July 18, 1991

To: Ed Erickson  
Jacquie Davidson  
Ted Dunham  
Allan Meyer

From: Ann Dinger  
Diane Wooden

Re: Typical KAO Dust Contamination and SOFIA Straylight Analysis

cc: Paul Davis (NASA-TM-110710) TYPICAL KAO DUST  
Paul Harvey CONTAMINATION AND SOFIA STRAYLIGHT  
Jerry Hirata ANALYSIS (NASA. Ames Research  
Ramsey Melugin Center) 7 p  
Ruben Ramos  
Gary Thorley  
Chris Wiltsee

N95-71655

Unclass

Z9/74 0060171

## Introduction

The scattering properties of the SOFIA mirrors are a critical part of the straylight analysis. The amount of scatter and the resultant straylight depend strongly on the amount of dust contamination assumed and its particle size distribution. The scattering decreases as the wavelength increases, because only particles with diameters near or greater than the wavelength scatter efficiently.

An mirror sample exposed during 20 KAO flights in the fall of 1990 is being used to determine realistic mirror scatter data for the SOFIA straylight analysis. The Al mirror sample with an 800Å SiO overcoat was provided by Allan Meyer. It was uncovered just before pre-cool and covered up just after cavity warmup on the KAO, and thus represents a particle size distribution relevant to flight conditions. Diane Wooden's dust counts on the test sample were described in a memo dated May 20, 1991. Photographs at 4 different magnifications, (macro, 10X, 110X, and 250X), were used to determine the number of particles per square centimeter in 24 distinct size ranges between .01 and 450µm. These counts have now been summed to determine the particle size distribution and the fraction of the mirror surface covered by dust. The results are compared to the standard surface contamination classes defined in MIL-STD-1246A.

## Method

For each size range, the number of particles per square centimeter was determined by averaging over the areas counted. As many as seven separate areas were counted in some size ranges; above  $20\mu\text{m}$  only one area of  $3.7\text{cm}^2$  was used. Below  $.24\mu$ , many of the particles appeared quite orange to the eye. These small particles appeared brighter and more numerous on the photographs taken without the Kodak 38A blue filter. Scott Sanford believes that they could be droplets of sulphuric acid and/or another sulphur compound from the atmosphere, which are strongly absorbing in the blue. Below  $.24\mu$ , only the photographs taken without the filter were used to determine the average number of particles per square centimeter.

The averages for each diameter range were then summed from the largest size to the smallest to determine the total number of particles per square centimeter with diameters greater than or equal to each size range. The results are displayed in Figure 1.

Out to  $20\mu\text{m}$ , the number of particles falls off smoothly with increasing diameter. Beyond this point, the small number of particles leads to a large amount of scatter. The final two points reflect one  $450\mu\text{m}$  diameter particle. The next point indicates 7 particles with diameters between 90 and  $135\mu\text{m}$ . The data beyond  $20\mu\text{m}$  could be improved by counting more of the mirror and increasing the number of size ranges.

The standard surface cleanliness classes are also plotted in Figure 1. Their particle size distributions are defined in MIL-STD-1246A. They have a power law fall-off of the number of particles per unit area above a given diameter as the diameter increases. At Class 1000, a surface has one particle per square foot whose diameter is greater than  $1000\mu\text{m}$ . These surface cleanliness levels are not the same as clean room classes, which describe the number of particles per unit volume of air.

The particle size distributions for the standard cleanliness classes exhibit an inflection below  $1\mu\text{m}$ . This inflection results from a discontinuity in the approximation used to calculate the numbers of particles, which involves the logarithm of the particle diameter. However, the uncertainty in this region is not important for determining either the total surface coverage to the infrared scatter.

The surface area covered by particles in each size range was calculated assuming spherical particles of the mean diameter. Most of the particles appeared nearly spherical. Realistically, each size range should contain more small particles than large. However, the larger particles have a greater area, which will tend to offset the skewing of the size distribution.

The surface coverage for each size range was calculated by multiplying the particle count by the projected area of a spherical particle of the mean diameter. These surface coverages were then summed from the largest size to the smallest to determine the total area covered

by particles with diameters greater than or equal to each size range. The results are displayed in Figure 2.

The fraction of the test sample surface covered by dust is 1.9%, which is slightly below the value for Class 750, and substantially below the Class 1000 coverage that is being used for the current straylight analysis. The surface coverages for the various classes are given below.

Contamination	Surface Coverage
Class 300	2.72E-4
Class 500	3.16E-3
Class 750	2.53E-2
Class 1000	1.23E-1
KAO Sample	1.90E-2

On the test sample, the fraction of the surface covered by dust larger than a specific diameter falls off slowly between 1 and 10 $\mu$ m. The slope is steeper at longer wavelengths. The substantial number of particles below 1 $\mu$ m do not contribute significantly to the surface coverage. In contrast, in the standard contamination classes, the fall-off of the surface coverage with increasing diameter begins near 5 $\mu$ m and rapidly becomes much steeper than the KAO distribution.

Figure 3 compares measurements of the emissivity of the test sample made by Marc Chate-laine of JPL before and after the 20 flights. He measured the reflection of an LN<sub>2</sub> bath with the sample at room temperature. The emissivities are estimated to be accurate to +/- 1%.

The horizontal lines in Figure 3 indicate the adopted near infrared means for the regions outside the emission lines. If the particles and the underlying mirror emitted as black bodies, the effective emissivity of the particles could be calculated from:

$$\epsilon_T = \epsilon_M * (1 - f) + \epsilon_P * f$$

where  $f$  is the fraction of the surface covered by particles, and  $\epsilon_T$ ,  $\epsilon_M$ , and  $\epsilon_P$  are respectively the emissivities of the dirty mirror, the clean mirror, and the particles. Substituting  $\epsilon_T = .0595$ ,  $\epsilon_M = .033$ , and  $f = .0190$  leads to the physically impossible result that  $\epsilon_P = 1.43$ . If there were no measurement errors, one would have to conclude that the emissivity of the underlying mirror increased by 25 to 30% in the year between the two measurements. However, the two measurements are consistent within the estimated errors. Since this calculation does not lead to an effective emissivity for the particles, a value of .95 will be adopted for future analyses.

## Current Straylight Analysis

The chopping analysis described in the memo of February 1, 1991 is proceeding. Three wavelengths are being used, 6, 12, and 100 $\mu$ m. The bandpasses are 2, 4, and 34 $\mu$ m, respectively. The emitting surface is the tropopause at 6 and 100 $\mu$ m, and the Earth's surface at 12 $\mu$ m. The straylight differences between the two halves of a full 8' chop in the elevation direction are being evaluated.

The opening in the fuselage and the aftramp have been added to the APART model of SOFIA, because they influence the amount of the Earth that can shine into the cavity. The final calculations will be performed with the APART's Broad Source Integration routine, which requires Program 3 output at 3 different azimuths, with 10 off-axis angles for each. Results for other azimuths and off-axis angles are interpolated. Use of the BSI routine allows the asymmetrical nature of the aftramp to be taken into account.

The mirrors have been assumed to have Class 1000 contamination, which makes them the most important straylight sources. Since the mirror scatter is proportional to the surface coverage, adopting the KAO contamination level would reduce the mirror scatter by roughly the factors below. The overall reduction in the straylight would be somewhat less, because diffraction and scatter off the secondary obscuration and the support struts would not be affected.

Wavelength	Coverage Decrease
6 $\mu$ m	13.2
12 $\mu$ m	18.4
100 $\mu$ m	12.9

## Next Analysis

The chopping analysis should be repeated using the KAO contamination level for the mirrors. Comparison of the results with KAO and Class 1000 contamination levels will allow straylight predictions to be made for other cleanliness levels. These predictions could be used to determine how often the SOFIA mirrors should be cleaned.

Both 6 and 12 $\mu$ m do not need to be repeated; the results at one of these wavelengths can easily be scaled to the other, as the scattering does not change much over such a small range in wavelength. The secondary mirror will probably not be as dirty as the primary and the tertiary. However, its scattering is not as important, as it is not directly illuminated by the Earth. It seems unnecessary to assign the secondary a different contamination level.

Figure 1

KAO DUST PER SQUARE CENTIMETER  
Above a Given Particle Size

vs

PARTICLE DIAMETER  
Microns

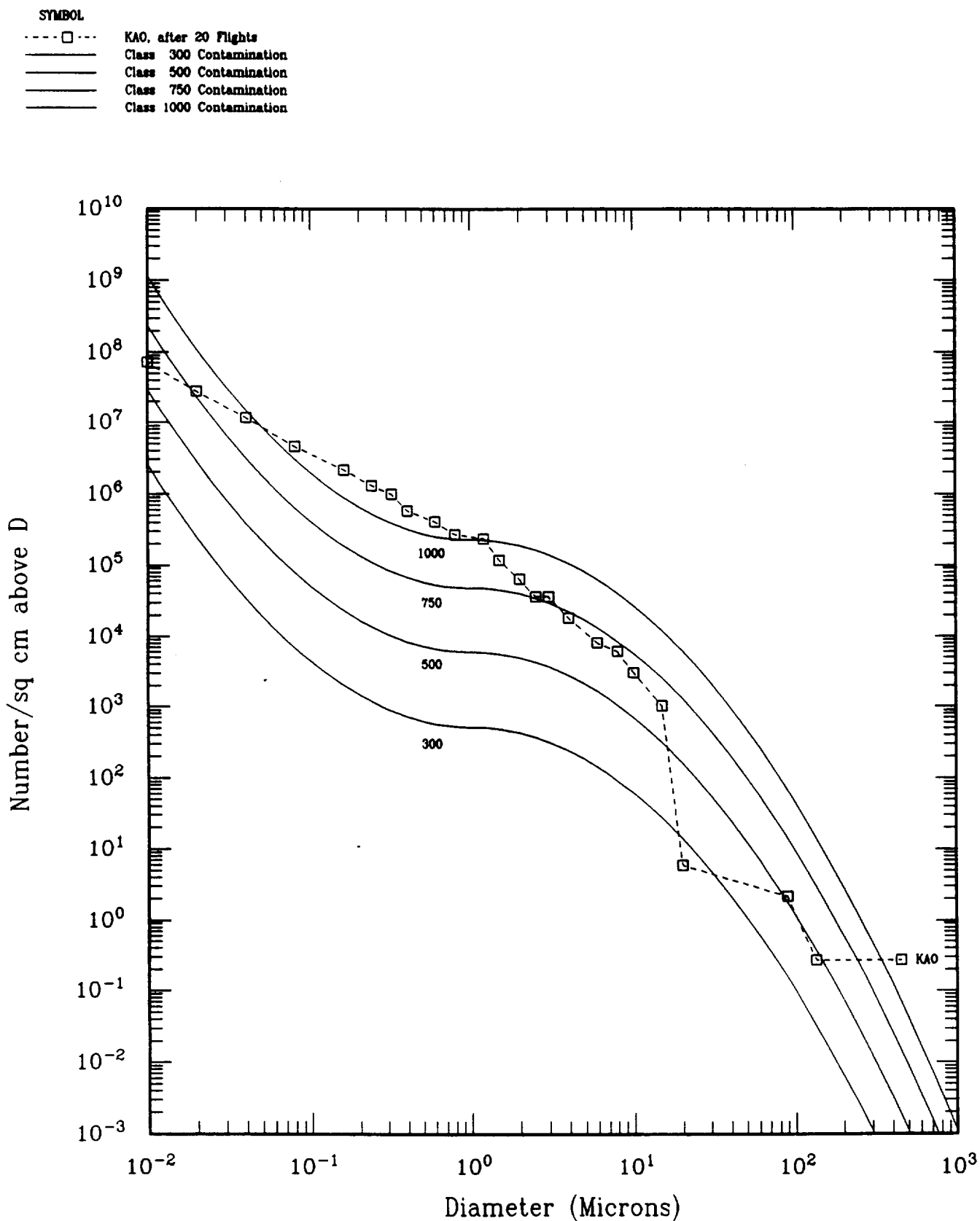


Figure 2

KAO DUST OBSCURATION FRACTION (20 FLIGHTS) vs PARTICLE DIAMETER  
Above a Given Particle Size Microns

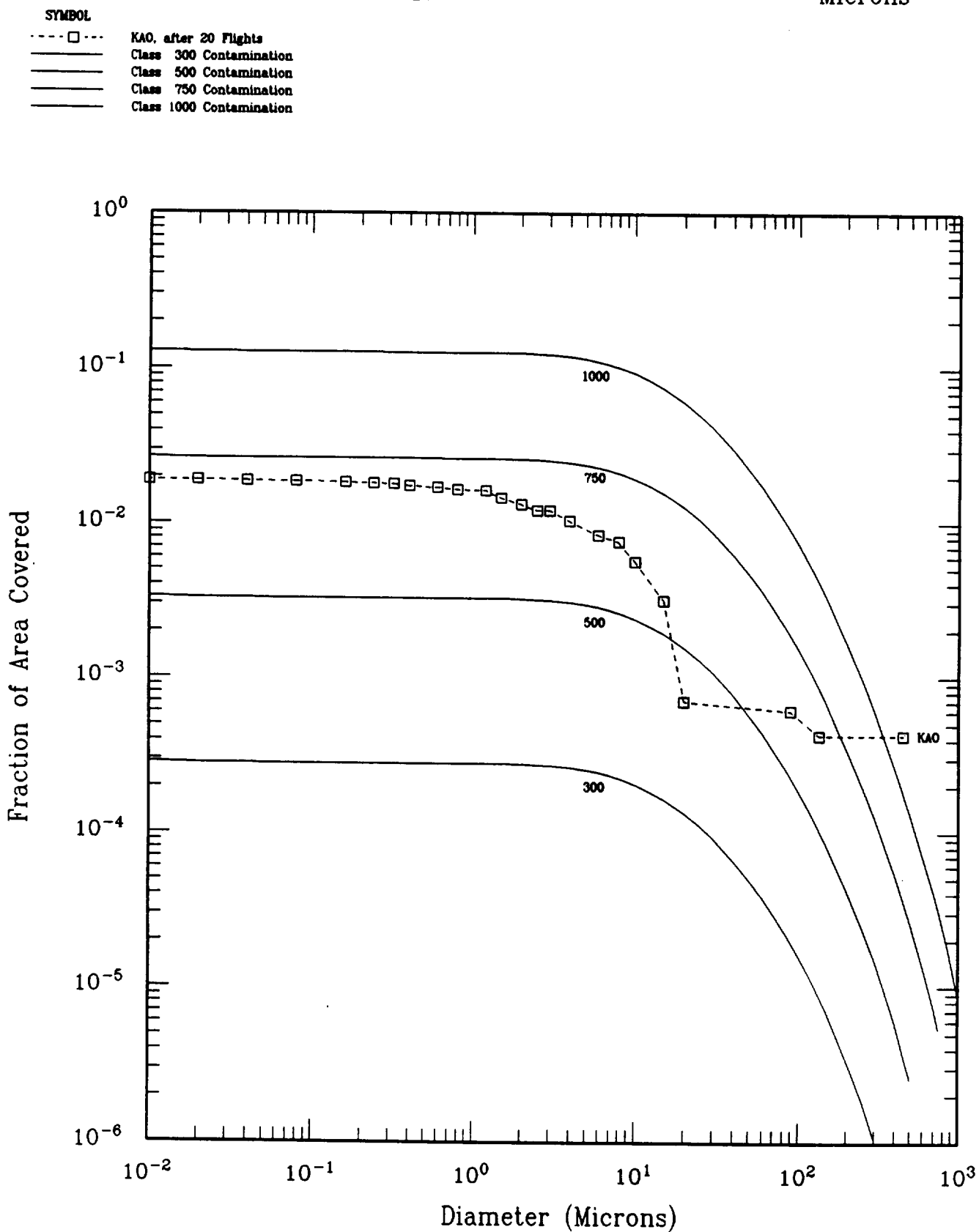


Figure 3

# MIRROR SAMPLE EMISSIVITY

Sample B: Aluminum + 800 Angstrom SiO

